# Mathematical and Computational Assimilation for Plasma Boundary Physics

Maria Chrysanthou†, S.T. Millmore, N. Nikiforakis
Laboratory for Scientific Computing, University of Cambridge

# Tokamak Energy & ST40

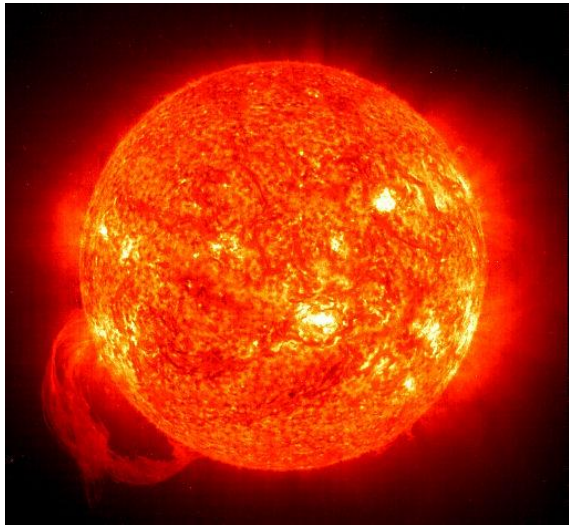

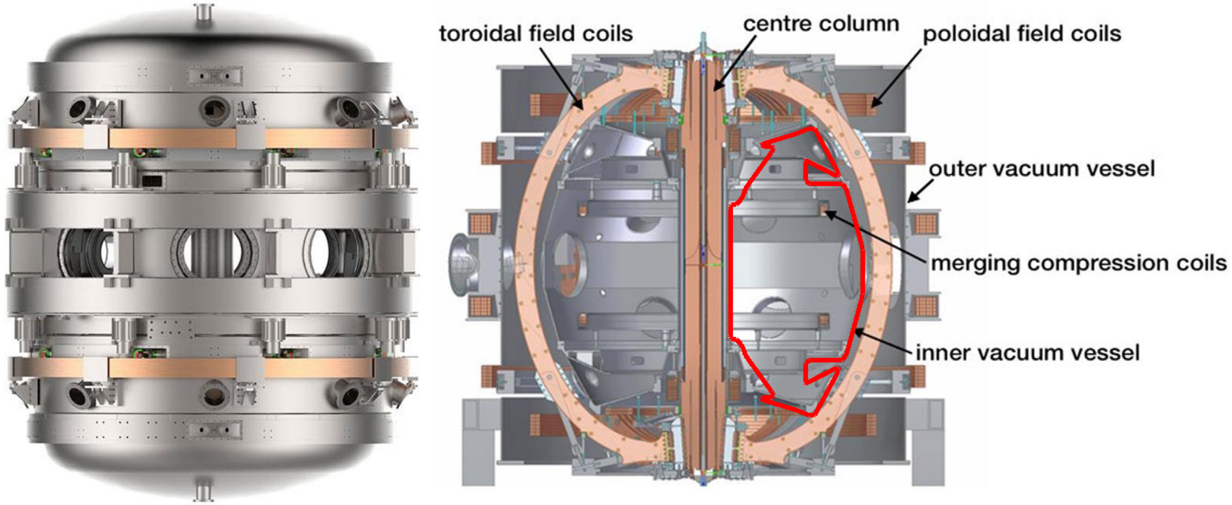


- Tokamak Energy aims to use nuclear fusion as a commercial energy source, which is clean, economic and easily deployable.
- Their approach is based on combining the increased efficiency of the spherical tokamak with high-field HTS magnet technology for improved confinement.
- The ST40 reactor is their compact spherical tokamak, a high-field and low aspect ratio device.

# Fusion Reactor Simulations: a challenging problem

**CHALLENGES:**
- Complex physics
- Disparate length- and time-scales
- Nonlinear interactions and feedback across scales
- Geometric complexity

**CURRENT APPROACHES:**
- Single physics modelling by separation of scales
- Partial physics integration by means of co-simulation
- Space discretisation by coordinate transformation

- Figure by PhD student, Alexander Farmakalides.

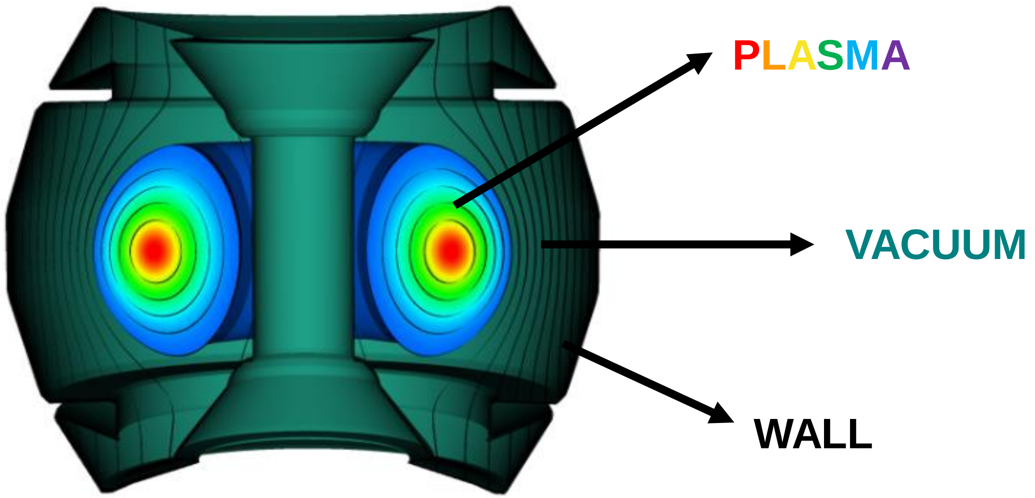


**OUR APPROACH:**
Integrated multi-physics simulations by employing multi-material/matter interface capturing methodologies, in a Cartesian frame of reference and making use of hierarchical AMR both in space and time.

# Plasma – Resistive Wall Formulation

- Resistive MHD model for plasma:

$$\frac{\partial \rho}{\partial t} + \nabla \cdot (\rho \mathbf{v}) = 0$$

$$\frac{\partial \rho \mathbf{v}}{\partial t} + \nabla \cdot \left( \rho \mathbf{v} \otimes \mathbf{v} + \left( p + \frac{1}{2} B^2 \right) \mathbf{I} - \mathbf{B} \otimes \mathbf{B} \right) = \mathbf{0}$$

$$\frac{\partial U}{\partial t} + \nabla \cdot \left( \left( U + p + \frac{1}{2} B^2 \right) \mathbf{v} - (\mathbf{v} \cdot \mathbf{B}) \mathbf{B} \right) = \eta \mathbf{J} \cdot \mathbf{J}$$

$$\frac{\partial \mathbf{B}}{\partial t} + \nabla \cdot (\mathbf{B} \otimes \mathbf{v} - \mathbf{v} \otimes \mathbf{B}) = -\eta \nabla \times \mathbf{J}$$

- Faraday's law for rigid body (N.M. Ferraro et al. [2016]):

$$\frac{\partial \mathbf{B}}{\partial t} = -\nabla \times (\eta_w \mathbf{J}), \qquad \mathbf{J} = \nabla \times \mathbf{B}$$

# Our Framework

- Solving equations in their conservative form using a **finite volume** approach.

- **Mesh generation** in a Cartesian framework which gives advantages around complex geometries.

- **Hierarchical adaptive mesh refinement** to ensure enough resolution both in space and time for capturing relevant physics.
  - Using underlying framework of AMReX package, originally developed at Lawrence Berkley National Laboratory.

- AMReX framework is **highly parallelisable** and can efficiently run on architectures of various sizes.

- **Material boundary conditions** incorporated using state of the art sharp and/or diffuse interface methods.

# Plasma – Vacuum – Wall

- The objective of this work is to account for all regions of the reactor (plasma, vacuum, wall) within the same simulation, which represents a significant departure from current segregated solutions.
- This is a very challenging task, so we start by independently considering the interaction at interfaces which require special attention.

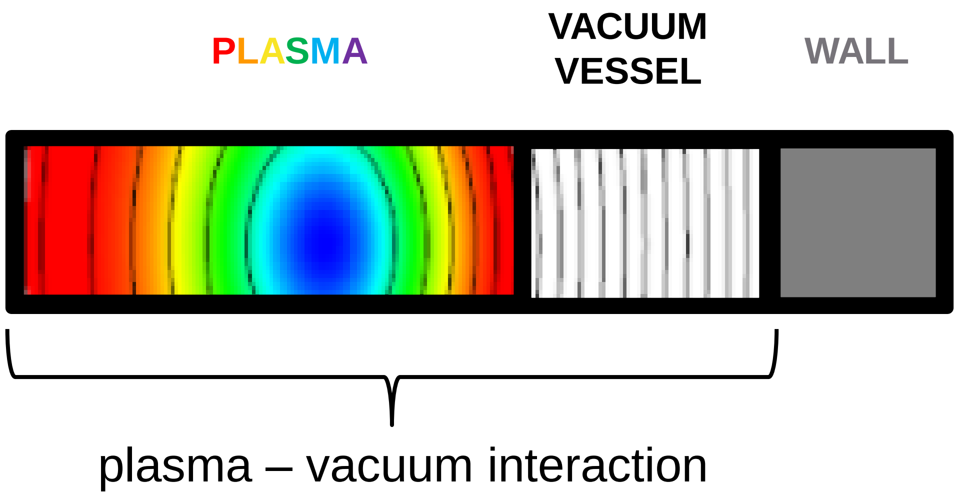

# Fluid – Vacuum Riemann Problem

- Even in its simplest form (one-dimensional, no magnetic fields), the fluid-vacuum RP is numerically very difficult to solve.
- Therefore, a major development of this work is the modification of the system of equations to enable realistic and physically consistent simulations of vacuum.
- The first step is to consider the exact solution for the vacuum RP in the presence of magnetic fields.

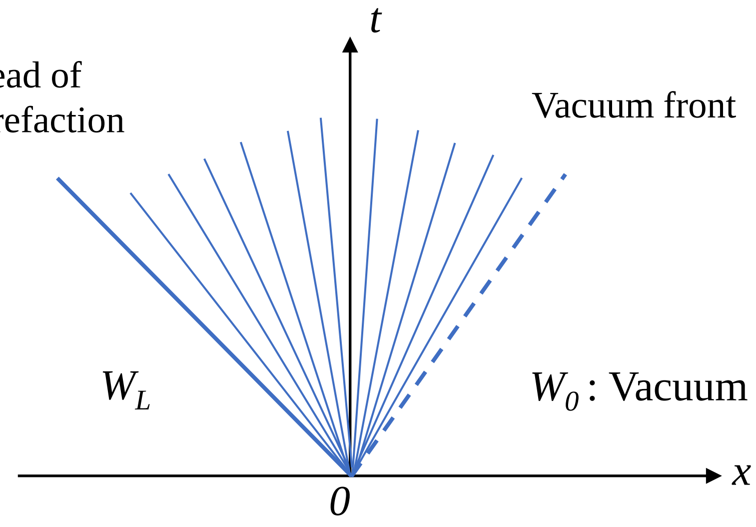


Figure: Riemann problem solution for a right vacuum state.

# MHD Exact Riemann Solver

- Developed an exact Riemann solver for one-dimensional MHD problems with unique solutions (following the work of Torrilhon [2002] and Takashi and Yamada [2014]).
- Enhanced the solver with the capability of solving Riemann problems with a vacuum initial state.

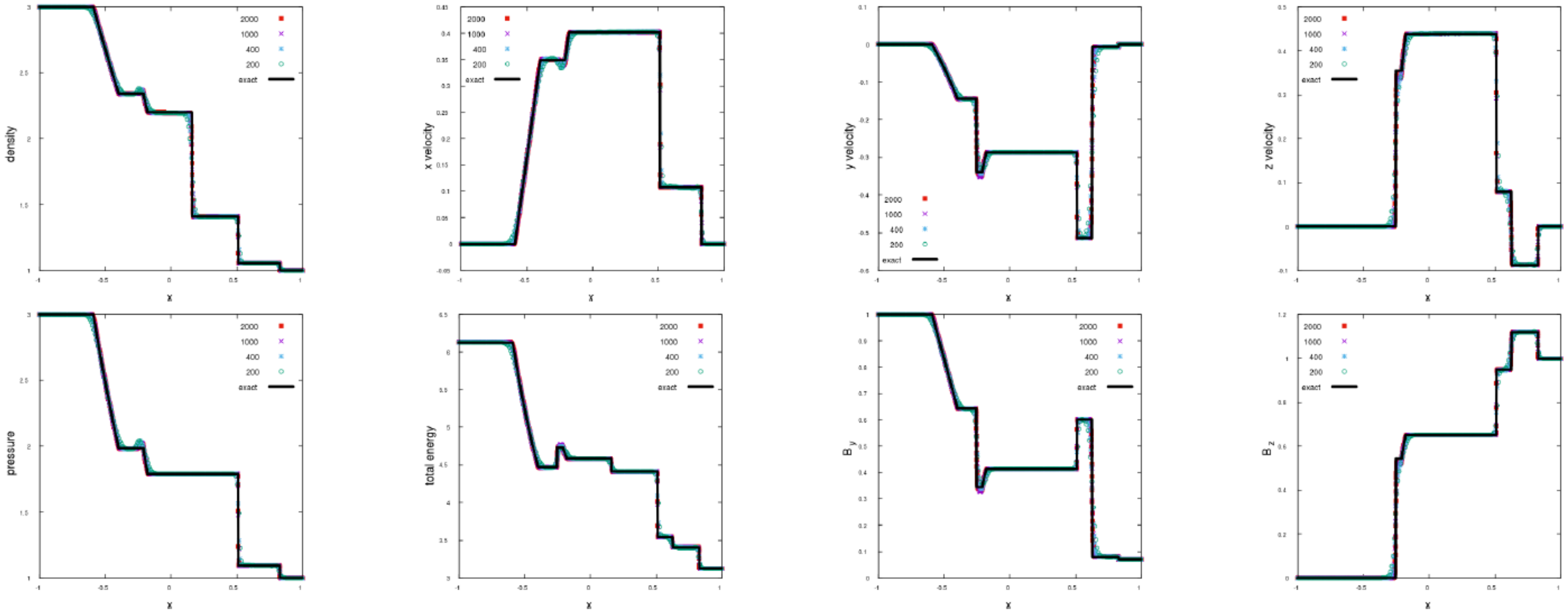

# Plasma-Void Riemann Problem

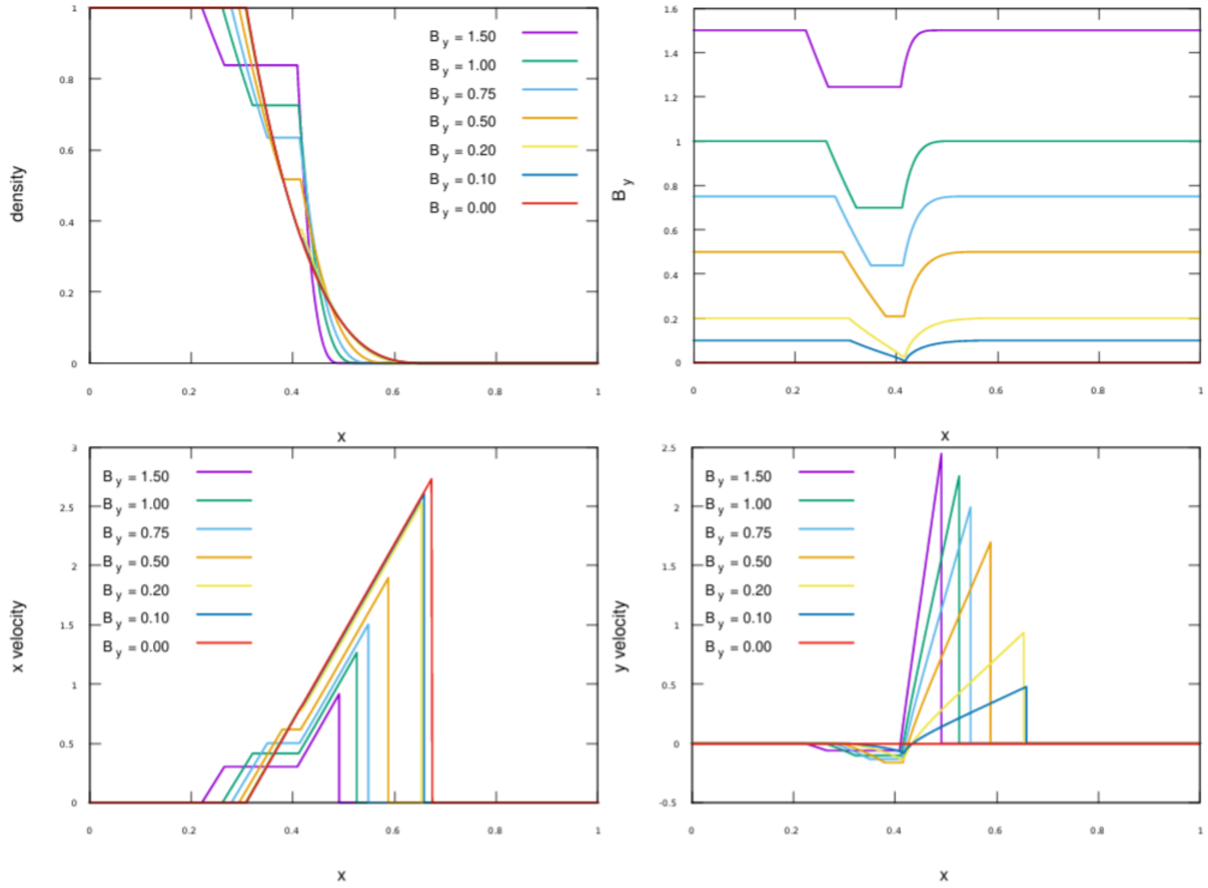


Figure: Exact solutions for plasma-vacuum Riemann problem, consisting of a fast rarefaction, a slow rarefaction and a contact wave at the plasma-vacuum interface.

| | $\rho$ | $v_x$ | $v_y$ | $v_z$ | $p$ | $B_x$ | $B_y$ | $B_z$ |
|---|---|---|---|---|---|---|---|---|
| Left | 1.0 | 0.0 | 0.0 | 0.0 | 0.5 | 0.375 | $(0.0, 0.1, 0.2, 0.5, 0.75, 1.0, 1.5)$ | 0.0 |
| Right | 0.0 | 0.0 | 0.0 | 0.0 | 0.0 | 0.375 | $(0.0, 0.1, 0.2, 0.5, 0.75, 1.0, 1.5)$ | 0.0 |

# Diffuse Void Interface Method

- We implement a novel diffuse interface method by Wallis *et al.* [2021] based on flux modifiers and interface seeding routines.
- This requires the introduction of a new evolution equation for the void volume fraction variable $\nu$.

$$\frac{\partial \nu}{\partial t} + \nabla \cdot \nu \mathbf{v} = \nu \nabla \cdot \mathbf{v}$$

- The entire system of equations is solved using an HLLC solver with MUSCL reconstruction on primitive variables, RK3 in time and a MUSCL-BVD-THINC reconstruction is also implemented for minimising numerical diffusion around the interface.
- Note, the presence of the non-conservative source term requires the adaptation of the update formula, which is now given by:

$$\nu_i^{n+1} = \nu_i^n + \frac{\Delta \mathrm{t}}{\Delta \mathrm{x}}\left(F_{i-\frac{1}{2}}(\nu) - F_{i+\frac{1}{2}}(\nu) + \nu_i^n\left(\nu^*_{x,i+\frac{1}{2}} - \nu^*_{x,i-\frac{1}{2}}\right)\right).$$

# Numerical Method

- Void seeding routine:
  1. In cells where $\nu \geq 0.9$, the void normal is calculated using Young's/ELVIRA method.
  2. A probe is sent along the normal and a new state $\boldsymbol{U}_{interp}$ is interpolated.
  3. If $\nu_{interp} < \nu$, a new state is defined, so that $\boldsymbol{U}_{new} = \boldsymbol{U}_{interp}$ .
  4. The new state is linearly combined with the original state, $\boldsymbol{U} \leftarrow (1-\nu)\boldsymbol{U} + \nu\boldsymbol{U}_{new}$ , but keeping the magnetic field variables and the void volume fraction variable constant.
- Flux modifier (improvement based on Munz's work [1994]):
  1. Cells are separated into three different types, fluid-fluid interface, fluid-void interface and void-void interface cells.
  2. Normal HLLC flux is computed for fluid-fluid interface cells and a modified flux is computed for fluid-void interface cells given by:

$$\boldsymbol{F}_{fi} = \begin{cases} \boldsymbol{F}_{fluid}^{HLLC} & \text{if } S_l \geq 0, \\ \dfrac{(S_r \boldsymbol{F}_{fluid}^{HLLC} - S_r S_l \boldsymbol{U}_{fluid})}{S_r - S_l} & \text{if } S_l < 0, \end{cases}$$

where $S_l = v_n^{fluid} - c_f^{fluid}$ and $S_r = v_n^{fluid} + \frac{2c_f^{gas}}{\gamma - 1}$ .

*fi*: fluid-vacuum interface

# Fluid Expansion into Vacuum Validation Cases

1. Unmagnatised fluid into unmagnetised void

2. Magnetised fluid into unmagnetised void

3. **Magnetised fluid into magnetised void**

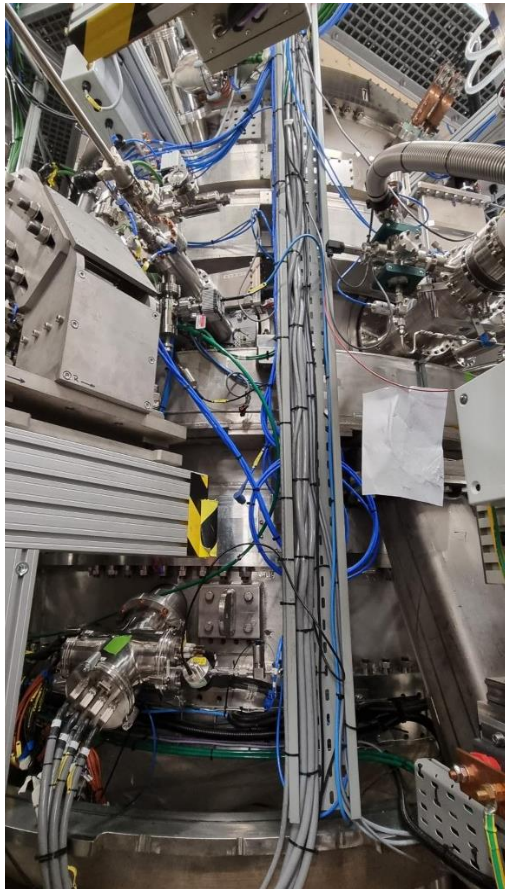

ST40 reactor, Tokamak Energy.

# 3. Magnetised Fluid – Magnetised Void

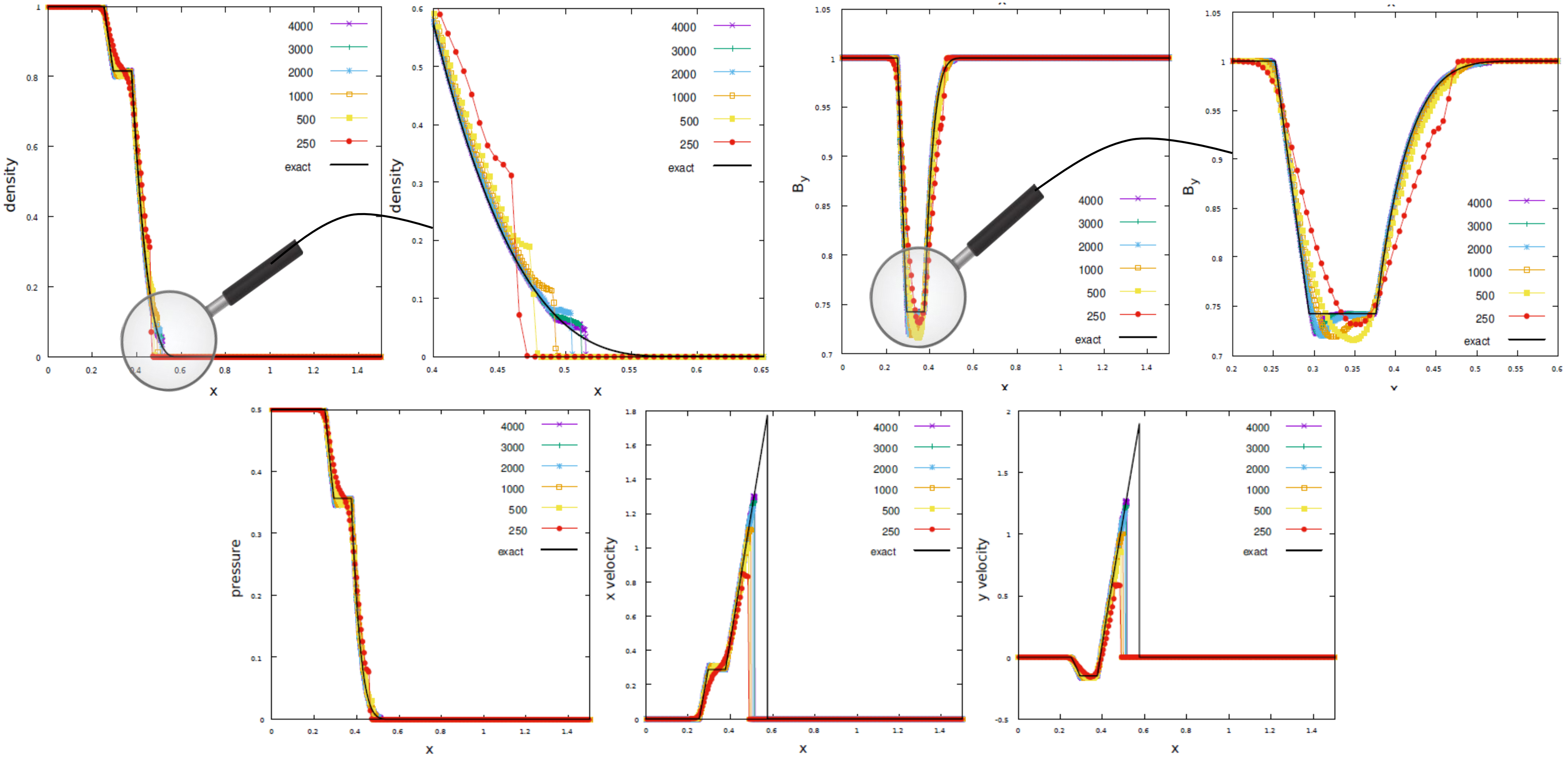


| | $\rho$ | $v_x$ | $v_y$ | $v_z$ | $p$ | $B_x$ | $B_y$ | $B_z$ |
|---|---|---|---|---|---|---|---|---|
| Test 3 Left | 1.0 | 0.0 | 0.0 | 0.0 | 0.5 | 0.75 | 1.0 | 0.0 |
| Test 3 Right | 0.0 | 0.0 | 0.0 | 0.0 | 0.0 | 0.75 | 1.0 | 0.0 |

# Adding a Rigid Body Model for the Wall

- As a first approximation, the vessel wall is treated as a rigid body (i.e. no electromagnetic or elastoplastic properties and no discretisation in that part of the domain).

- In the following results, we use a Riemann rigid body ghost fluid method (GFM) with perfectly conductive boundary conditions for the magnetic field.

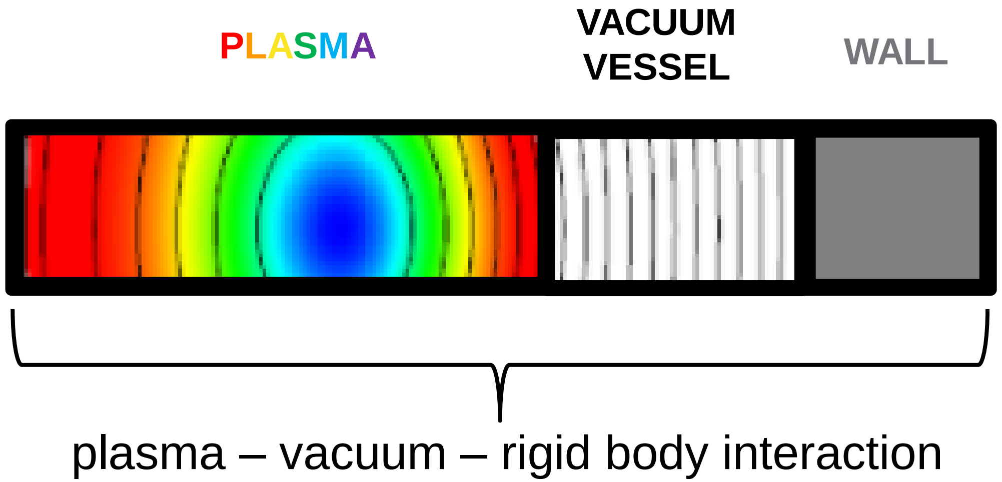

# Plasma Expanding into Vacuum within ST40 Geometry

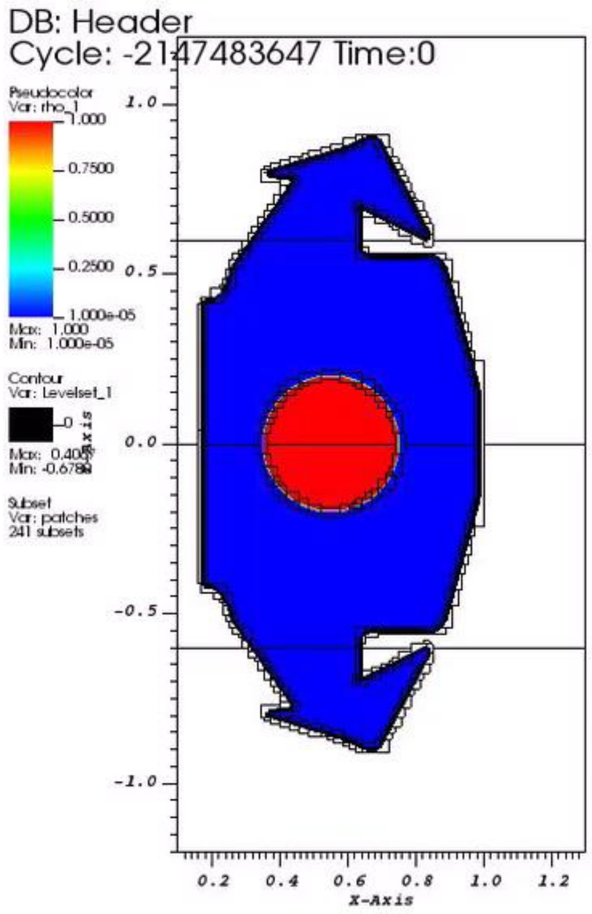


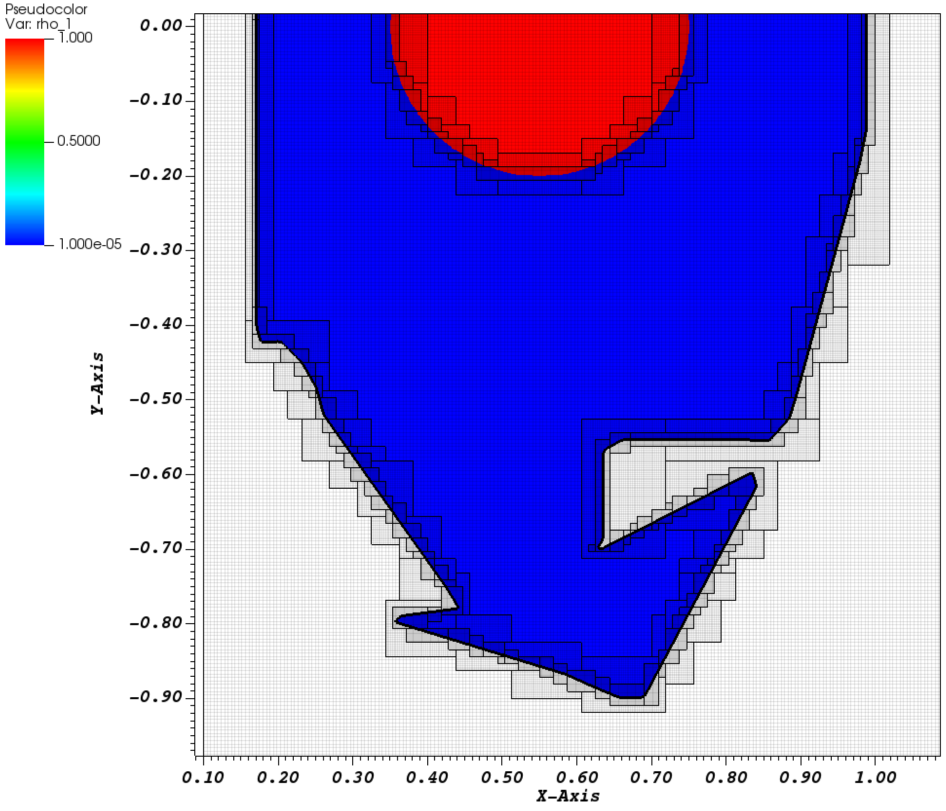


Figure: Employing AMR to increase resolution around material boundaries and sharp gradients.

# Adding a Resistive Wall Model

- We now take into consideration the resistive properties of the wall and enable discretisation within the rigid body part of the domain.

- The following equation now becomes important as it accounts for the evolution of the magnetic field within the wall, where $\eta_w$ is the resistivity of the wall.

$$\frac{\partial \boldsymbol{B}}{\partial t} = -\nabla \times (\eta_w \boldsymbol{J}), \qquad \boldsymbol{J} = \nabla \times \boldsymbol{B}.$$

# Cylindrical Equilibrium

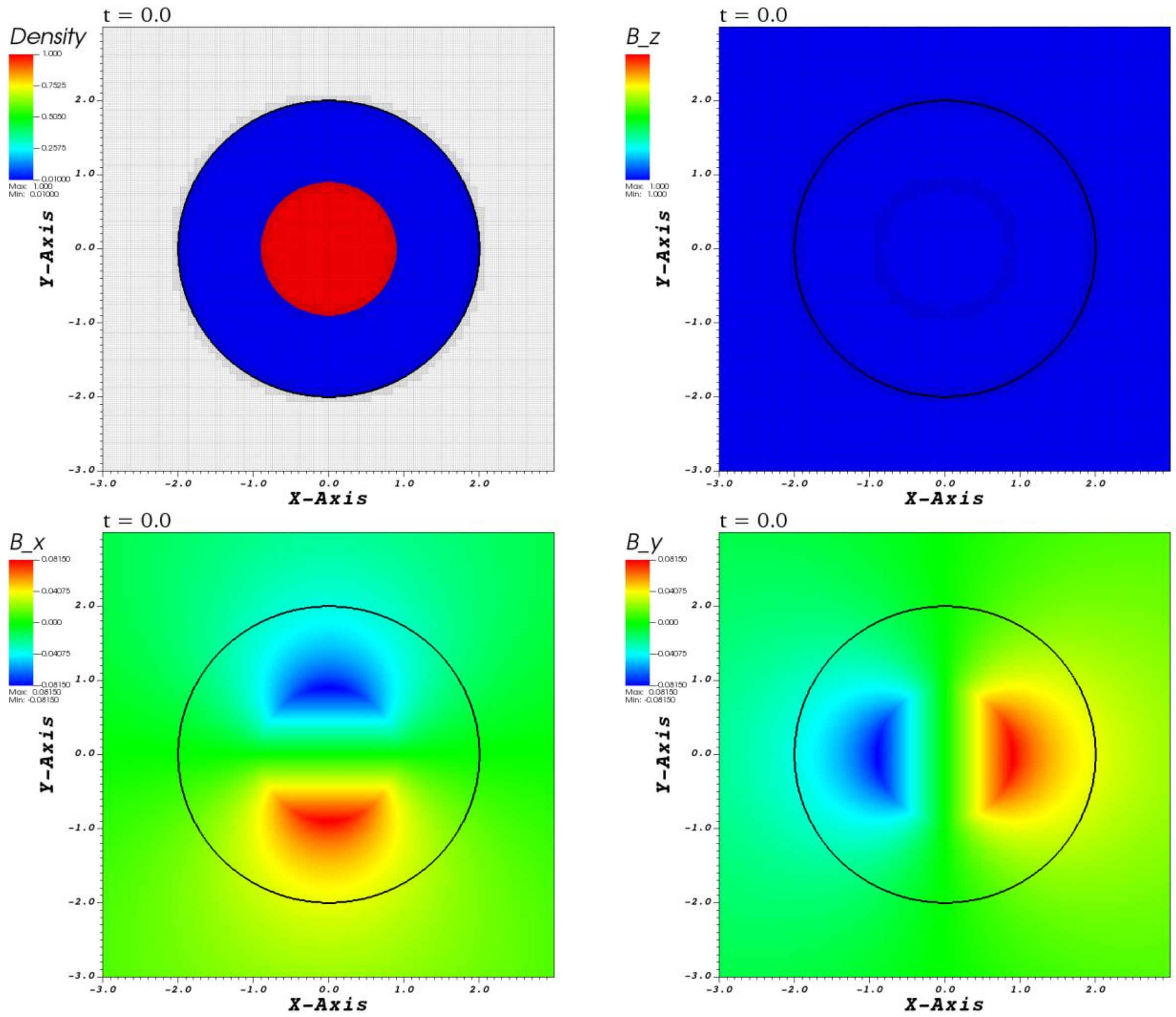


**Initial Perturbation**

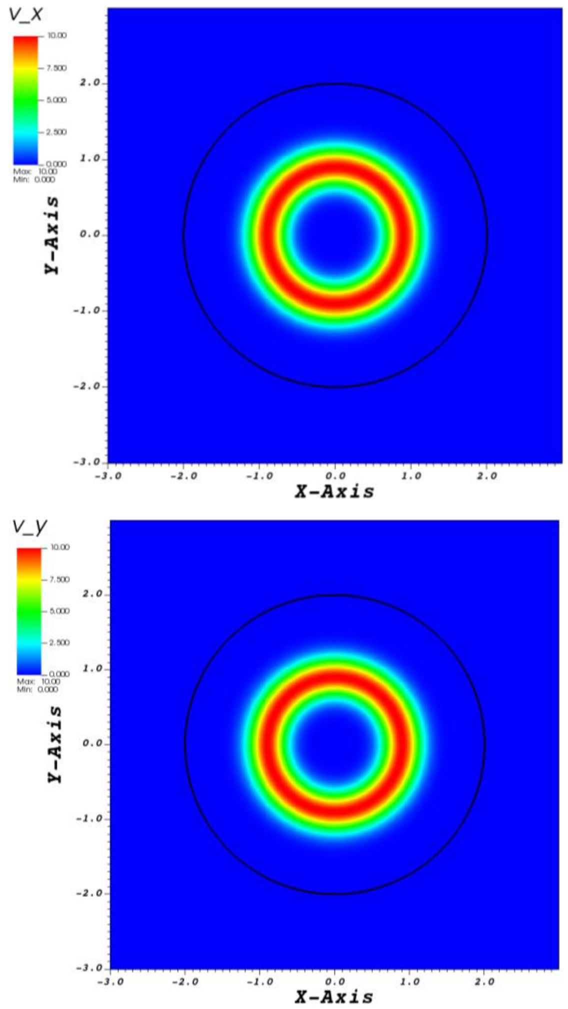

# Perfectly Conductive vs Resistive Wall

**PERFECTLY CONDUCTIVE**

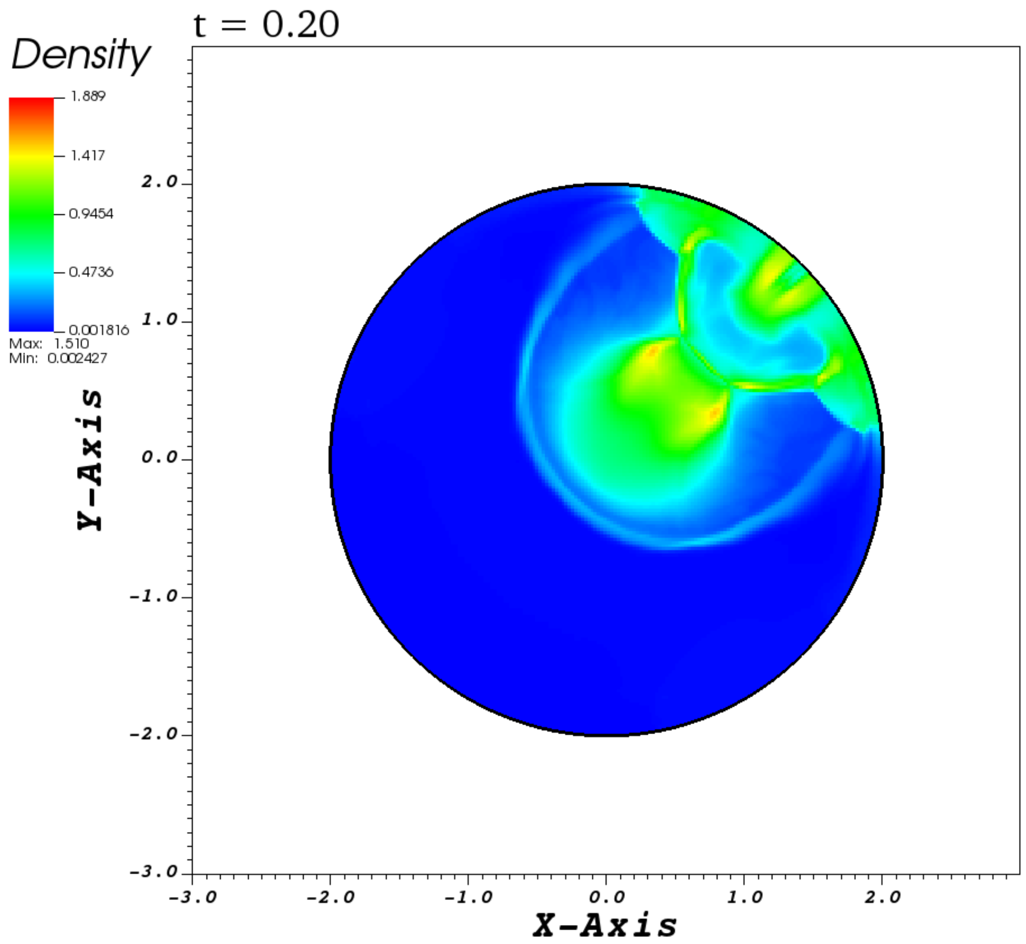


**RESISTIVE**

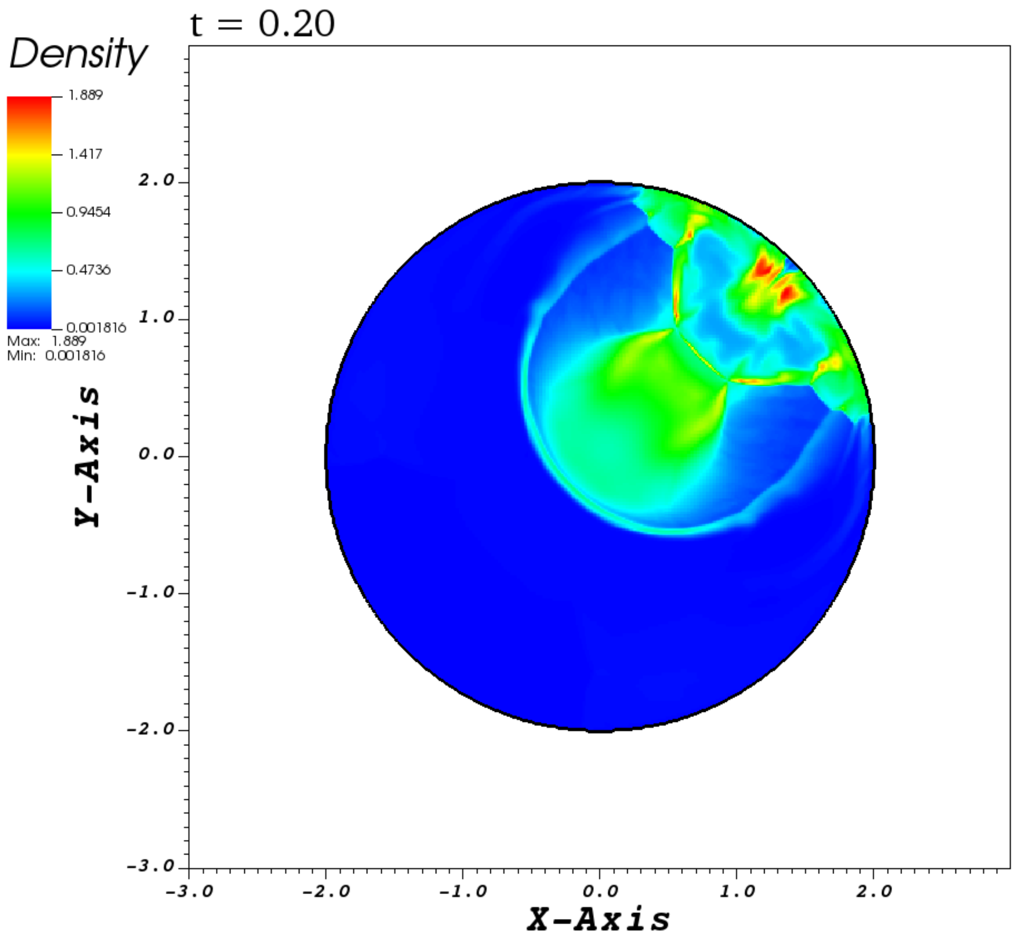


UNIVERSITY OF CAMBRIDGE

Tokamak Energy

# Perfectly Conductive vs Resistive Wall

## PERFECTLY CONDUCTIVE

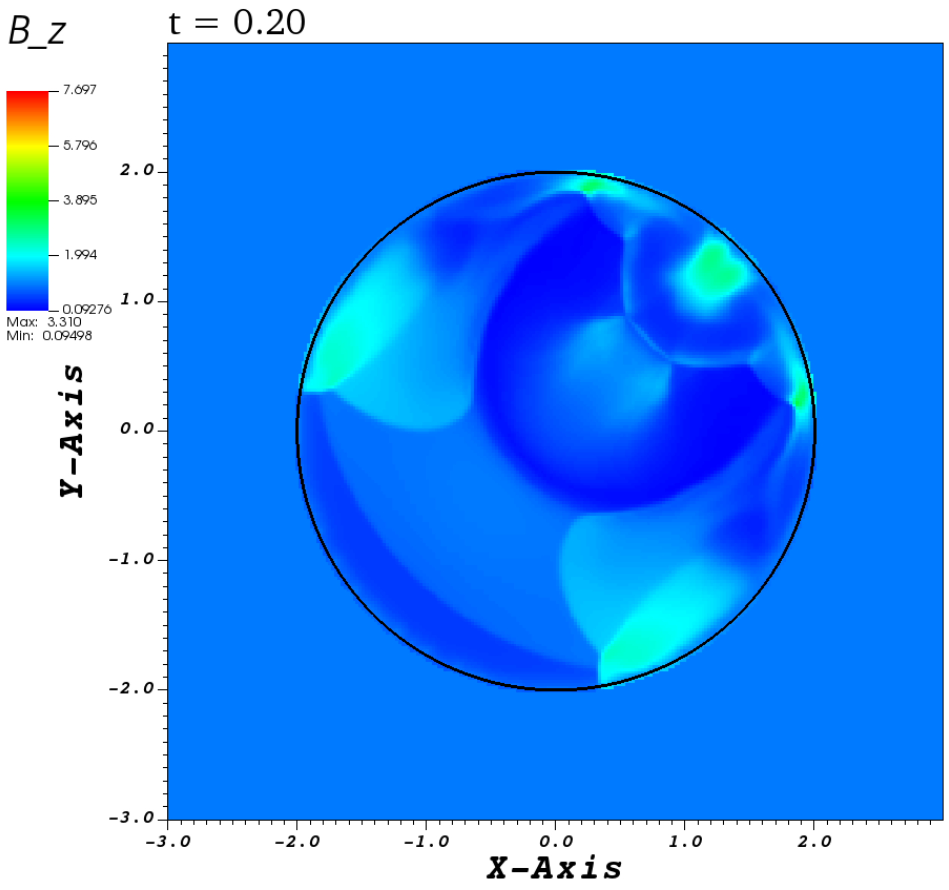


## RESISTIVE

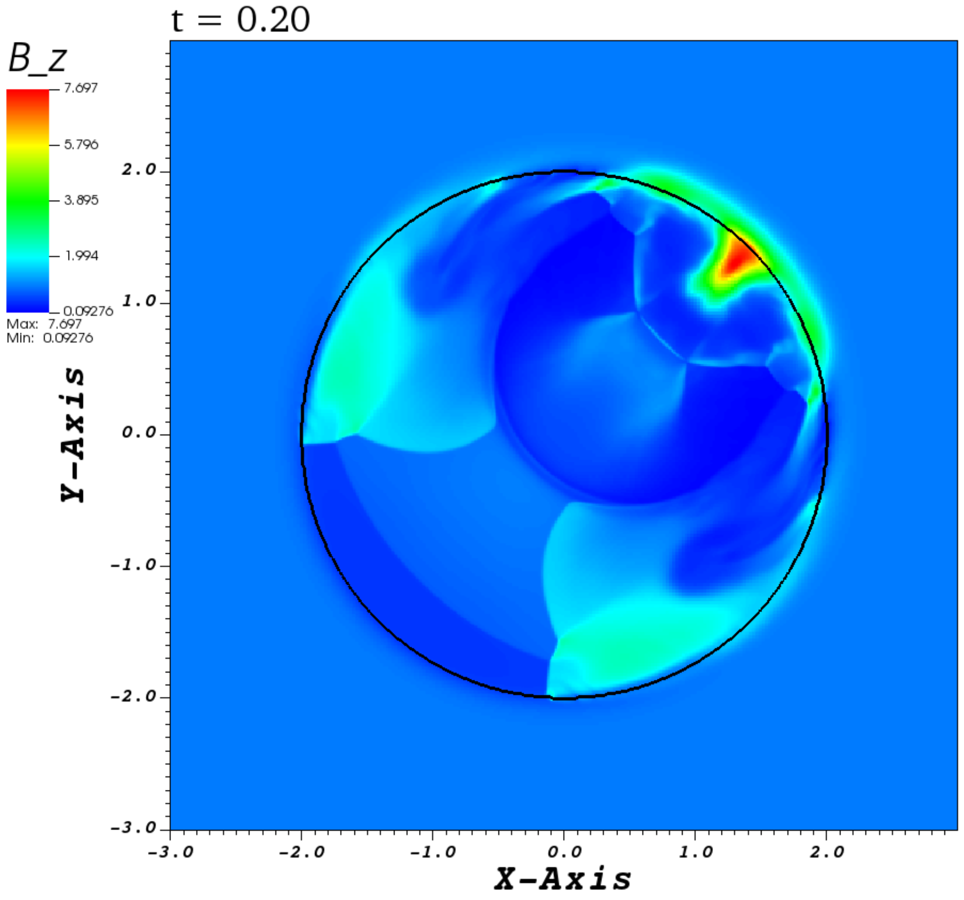


UNIVERSITY OF CAMBRIDGE

Tokamak Energy

# ST40 Geometry with Resistive Wall

| PERFECTLY CONDUCTIVE | RESISTIVE |
| --- | --- |

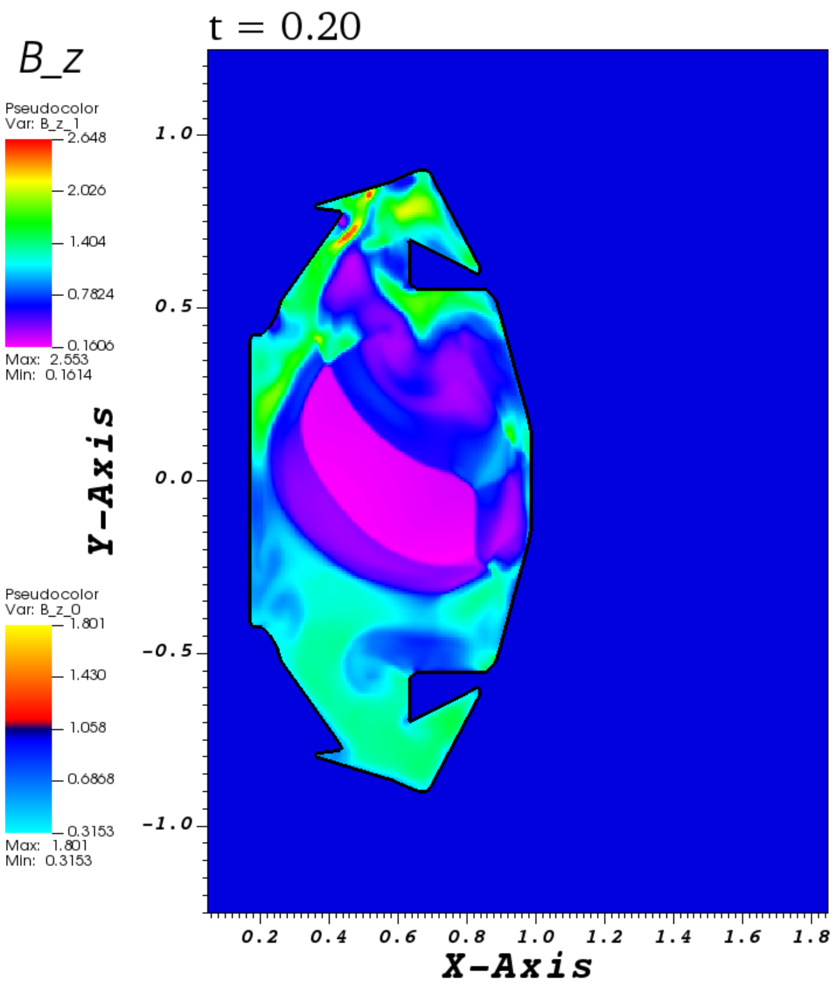


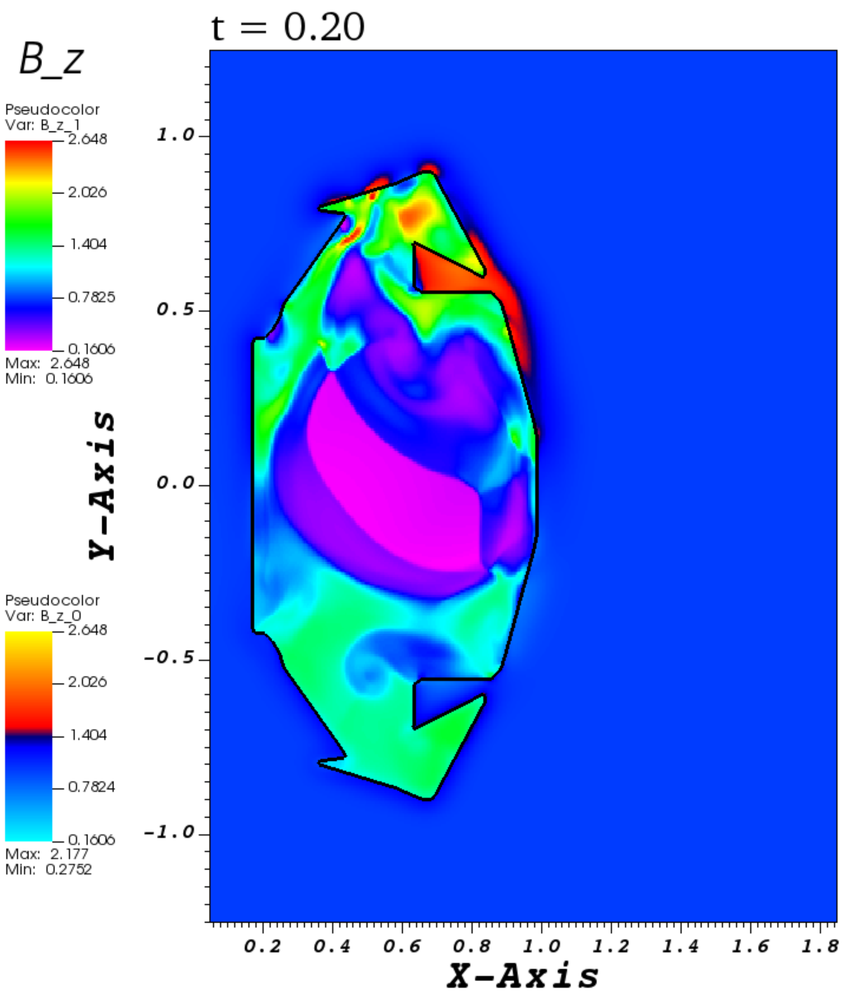

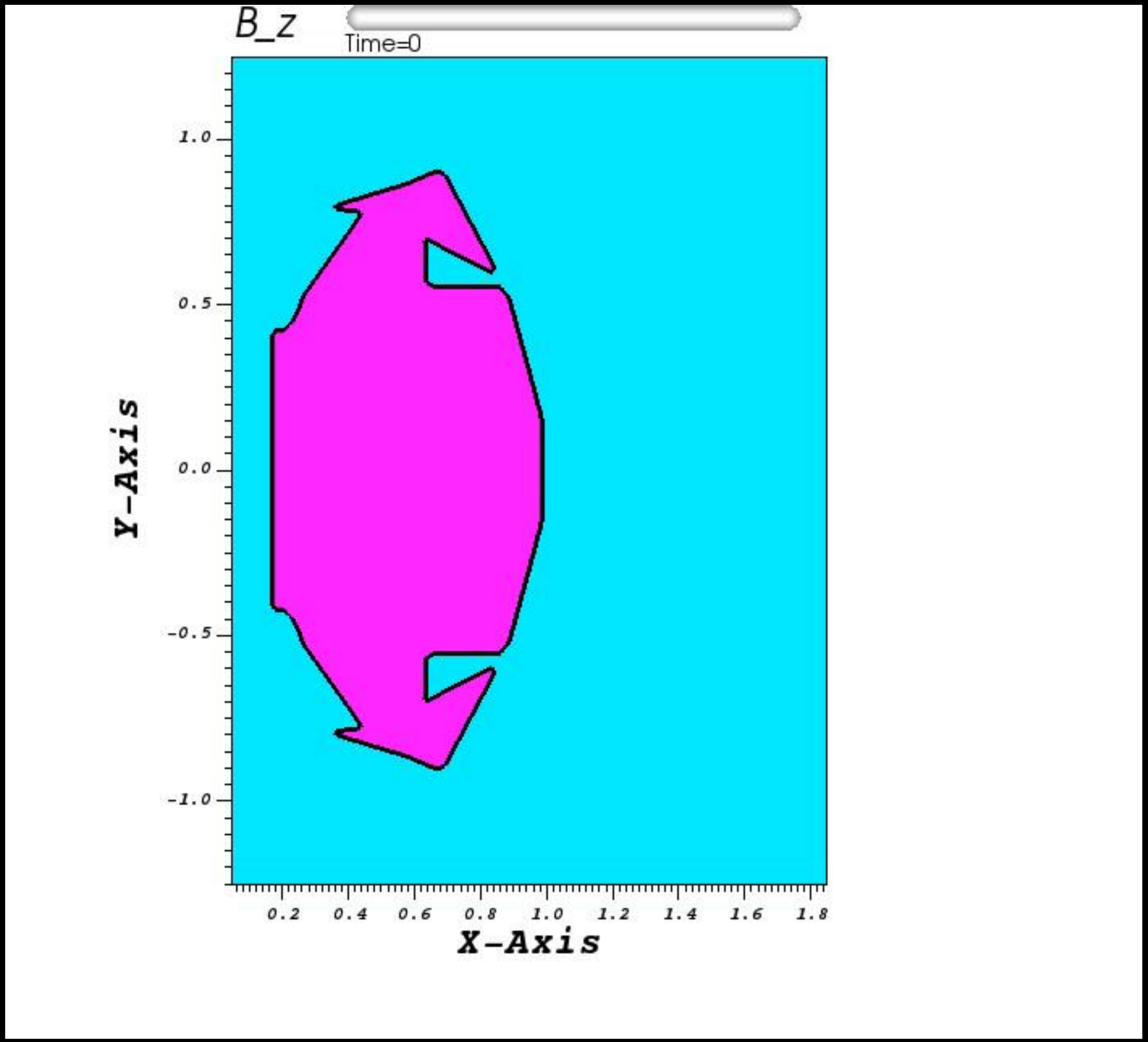
B_z
Time=0
Y-Axis
X-Axis
1.0
0.5
0.0
-0.5
-1.0
0.2
0.4
0.6
0.8
1.0
1.2
1.4
1.6
1.8

# Validation for Resistive Wall Model – Cylindrical Equilibrium

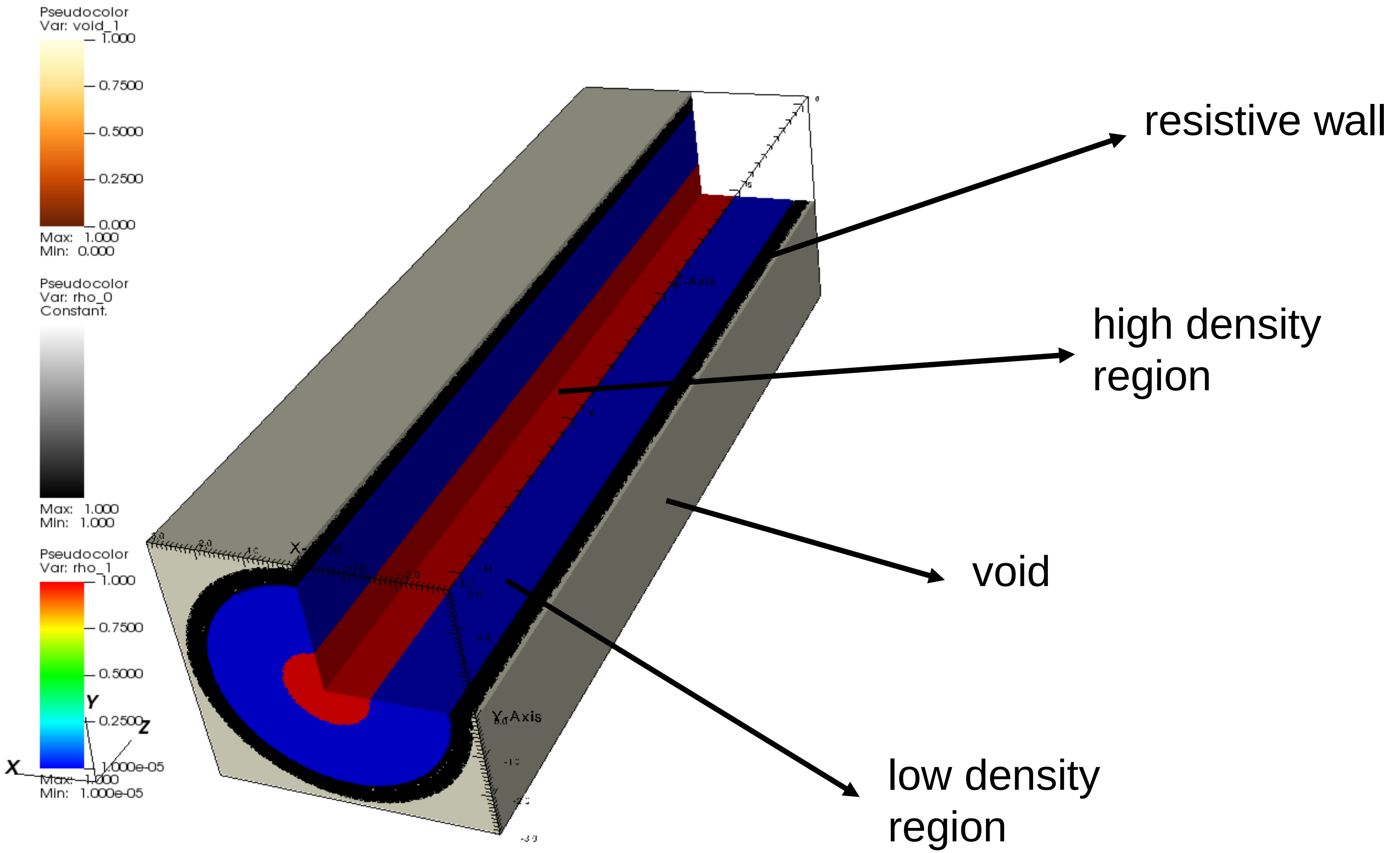

# Stability Analysis

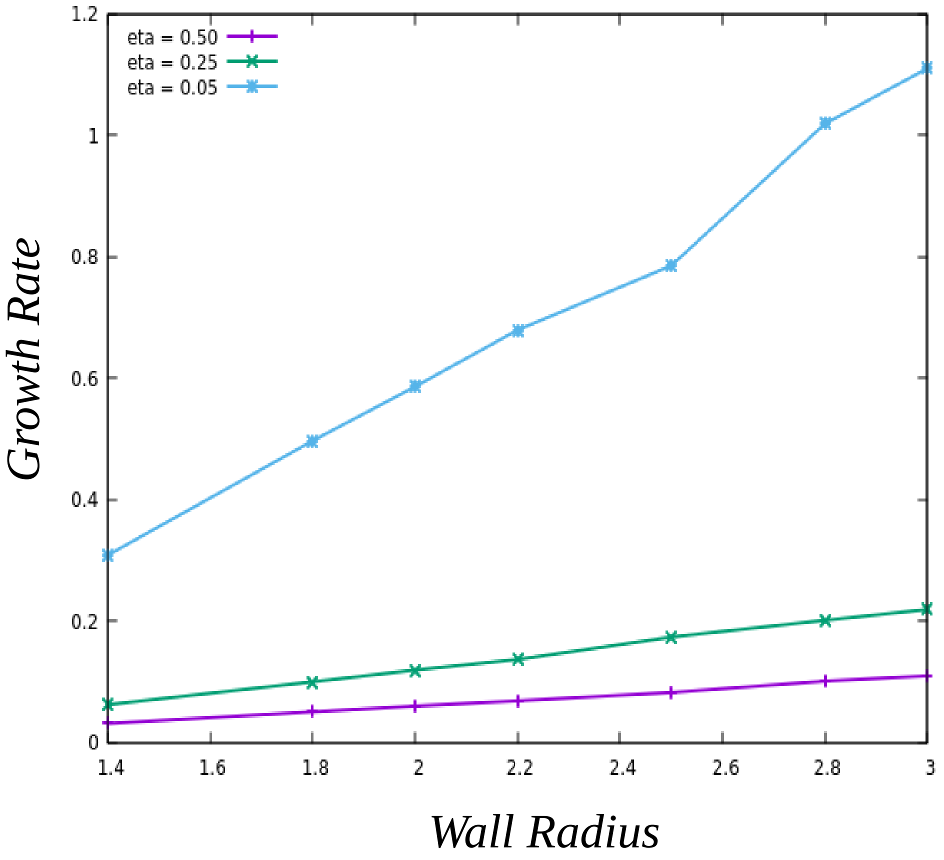


Figure 1: Instability growth rate plotted for different wall radii and wall resistivities.

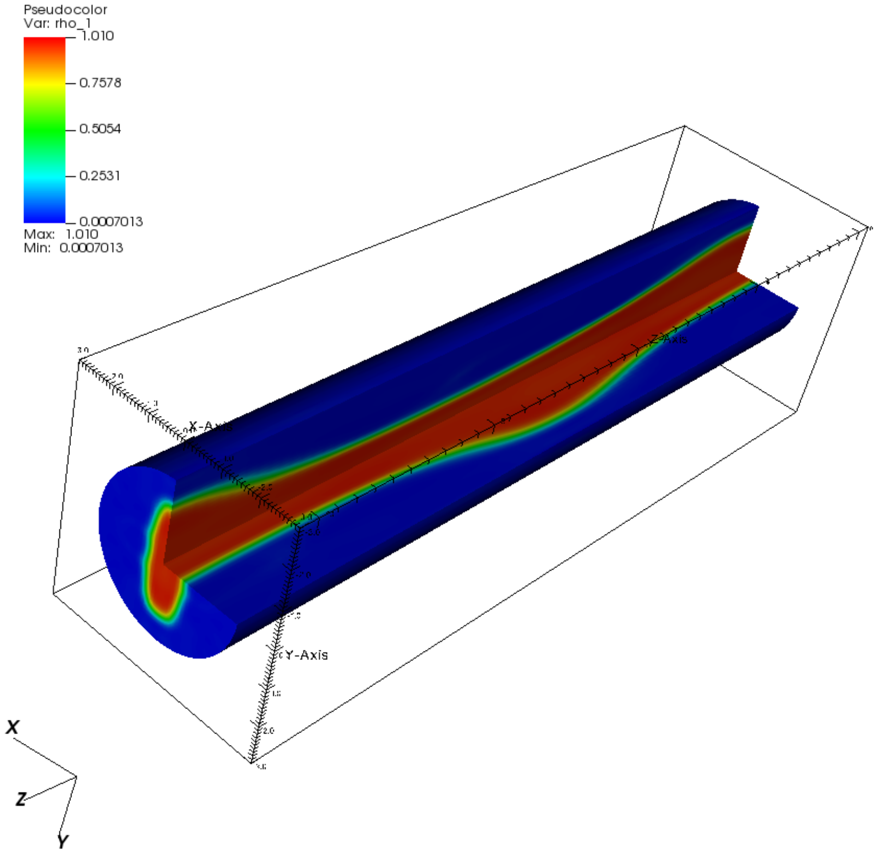


Figure 2: Density profile after a periodic perturbation was applied along the *z* and radial directions.

# Concluding remarks

- Making progress towards the development of a fully integrated model for whole-system fusion reactor simulations.
- Considering alternative methodologies for the accurate and physical representation of the vacuum vessel.
- Incorporating the electromagnetic properties of the confinement wall.

- Addition of more physics (full model) :
  - Multi-species system
  - Kinetic closure relations
  - Elastoplastic reactor wall model (for computing heat loads on divertor)
- Consideration and validation of unstable events within fusion reactors (e.g. ELMs and VDEs).